RSC Advances

ROYAL SOCIETY OF CHEMISTRY

www.rsc.org/advances

RSC Advances

PAPER

# The Initial Adsorption Process of Benzene in Double-walled Carbon Nanotubes Studied by In-situ Solid-state NMR

Received 00th January 20xx,
Accepted 00th January 20xx

DOI: 10.1039/x0xx00000x

**www.rsc.org/**

Wanling Shen,[a,*] Xin Li[a,*] and Hongbo Zhang[b]

Information of adsorption and diffusion in nanoporous material is helpful to fundamentally understand nanocatalysis and gas sensor. In this work, the adsorption process of benzene in double-walled carbon nanotubes (DWNTs) at the very earliest stages was directly monitored for the first time by using in-situ solid-state $^{13}C$ NMR. The results indicate that benzenes in and out of DWNTs can be conviniently distinguished by $^{13}C$ MAS NMR. The kinetics of the adsorption process was obtained by integrating the $^{13}C$ peaks as a function of adsorption time. The kinetic could be interpreted with a model of opposing adsorption-desorption process and the kinetic curves could be satisfyingly fitted by an exponential function.

## Introduction

Carbon nanotubes (CNTs) have triggered wide research interest in recent years for their graphitized walls and one-dimensional tubular morphology with unique electrical and mechanical properties.[1, 2] On the basis of their superior electrical and thermal conductivity and large surface area with pore diameters varying from one to tens of nanometers, CNTs have been used as adsorbents in water treatment and gas sensors for emissions such as NO, $NO_2$, CO, $CO_2$ and $SO_2$ from fossil fuel burning.[3, 4] CNTs also have been employed as support structures with metal or metal oxide catalysts located on the surface to facilitate better performances than conventional supports.[5] Furthermore, the curvature of CNT walls causes the π electron density of the graphene layers to shift from the concave inner to the convex outer surface, which results in a unique confinement effect and the molecules on the exterior walls of CNTs display different properties and chemical reactivities from those confined within CNTs.[6, 7] Molecules such as $H_2$, alkanes, alkenes, and carbon tetrachloride have been reported to bind more strongly on the interior surface of CNTs.[8, 9] It is also found that the adsorption of benzene can be enriched inside CNT channels so as to enhance the hydroxylation of benzene to phenol.[10] Besides being used as catalyst supports, CNTs itself has been reported to catalyze oxidative dehydrogenation of ethylbenzene to styrene and n-butane to butane.[11, 12]

Collectively, when CNTs are used as gas sensor or catalysts, the graphitized wall and well-defined channels create a novel confinement environment for guest materials, hence the adsorption and diffusion behaviors of guest molecules in CNTs are important for the sensing and catalysis performance. Studying the dynamic and kinetics of adsorption and diffusion of small molecules in CNTs will be helpful to deeply understand the mechanism of confinement effect of CNTs. However, it is challenging to study fast adsorption and diffusion processes in CNTs for many commonly applied analytical techniques. Solid-state NMR provides a possible way to study such a heterogeneous system. Pulsed-Field Gradient (PFG) NMR has been widely used to study the diffusion of guest molecules in porous materials such as zeolites,[13-15] but it does not allow the earliest stages of adsorption process to be probed. Bao et al. have applied in-situ continuous-flow laser-hyperpolarized $^{129}Xe$ MAS NMR to study the adsorption and reaction kinetics of methanol in CHA zeolites.[16] However, it is an indirect method. Harris et al. have proposed an in-situ capillary-breaking method enabling the very earliest stages of the adsorption process to be probed directly.[17, 18] In the method, spinning compresses the powder sample onto the inner wall of the rotor and create an empty region at the center of the rotor. A thin-walled glass capillary tube containing the liquid reagent is inserted into the void and then broken by spinning. Adsorption of the released reagent into the porous host material thus occurs and is directly recorded by NMR spectra from the earliest stages of the adsorption process (scheme 1). As to a benzene and CNTs system, some advantages make it suitable to employ an in-situ capillary-breaking $^{13}C$ NMR method to probe the initial adsorption process. First, to well distinguish signals of guest molecules in and out of the pores of host materials is the prerequisite to quantitatively study the initial adsorption process. The $^{13}C$ chemical shift of guest molecules in CNTs pores exhibits a large upfield shift due to the strong spatial diamagnetic shielding effect from ring currents induced by the delocalized electrons of nanotubes under the influence of external magnetic field.[19-27] The guest molecules out of CNTs pores are also shielded but to a lesser extent. As a result, it is easy to differentiate the $^{13}C$ peak of benzene

---

[a] College of Chemistry and Chemical Engineering, Henan University of Technology, Zhengzhou 450001, P. R. China.
[b] State Key Laboratory of Catalysis, Dalian Institute of Chemical Physics, Chinese Academy of Sciences, Dalian 116023, China.
* Corresponding author. Fax: +86037167756715E-mail: wshen@haut.edu.cn xinli@dicp.ac.cn

† Electronic Supplementary Information (ESI) available: [TEM image of an isolated DWNTs]. See DOI: 10.1039/x0xx00000x

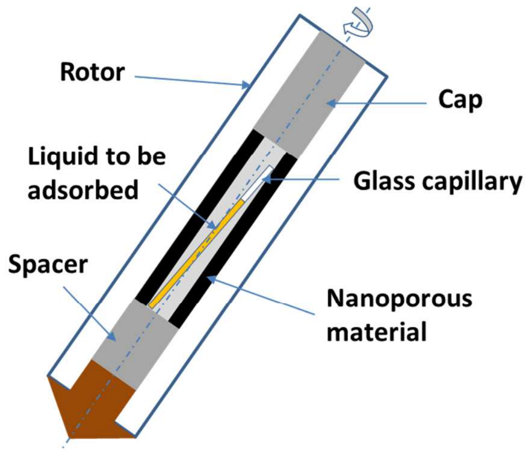

**Scheme 1.** Schematic illustration of the setup for the in-situ adsorption experiment inside the solid-state NMR rotor.

in CNTs pores from that out of pores, which is difficult in the case of other porous materials, such as zeolite and metal oxide. Second, the initial adsorption of benzene in CNTs is a fast process. It demands that the time interval between two in-situ collected NMR spectra should be short enough, which means a large number of scans to accumulate the spectra is not permitted, thus the NMR sensitivity of the guest molecule should be relatively high. The $^1$H nucleus has the highest NMR sensitivity among all kinds of nuclei, but the tuning range on $^1$H channel of NMR probes is relatively narrow. The “tuning and match” procedure for $^1$H channel before NMR measurement always failed on many commercial probes since the $^1$H resonance frequency always deviates severely due to the large magnetic susceptibility of CNTs samples. In contrast to the $^1$H channel, $^{13}$C channel has a relatively broad tuning range and the “tuning and match” procedure can be successfully completed on CNTs samples. Furthermore, if isotope-enriched benzene-$^{13}C_6$ were used, the six chemical shift equivalent $^{13}$C nuclei in every benzene molecule will bring a relatively high NMR sensitivity. Third, fast in-situ NMR measurements demand a short spin-lattice relaxation time ($T_1$) of the observed nuclei. The $^{13}$C $T_1$ of benzene, which varies from several to more than ten seconds in normal systems, can be largely decreased to as short as one hundred milliseconds in CNTs systems due to large spatial magnetic inhomogeneity, magnetic susceptibility anisotropy, demagnetizing field, defects and impurities in CNTs and the unique confinement effect of CNTs.[28-33]

Taking advantage of the benefits above, we studied the adsorption process of benzene in double-walled carbon nanotubes (DWNTs) at the very earliest stages by using the in-situ capillary-breaking $^{13}$C NMR method and interpreted the kinetic process, which will help to deeply understand the behavior of guest molecules and the confinement effects in the host nanoporous CNTs materials.

## Experimental section

### Sample preparation

The synthesis and purification of DWNTs follows the procedures described in the literature.[34] The 99% benzene-$^{13}C_6$ was purchased from Sigma-Aldrich Corporation.

Purified DWNTs sample was first dehydrated at 450°C for 16 h, followed by cooling to room temperature (RT). Benzene was then condensed and frozen inside the DWNTs sample with liquid nitrogen. The sample was equilibrated for 30 min at RT and packed into NMR rotors with a Kel-F endcap under a $N_2$ environment.

The details for in-situ capillary-breaking $^{13}$C NMR experiment were as follows: About 12 µl benzene was flame-sealed in a glass capillary tube. The capillary was then put into the zirconium oxide rotor. About 60 mg DWNTs dehydrated in advance was subsequently put into the rotor which was then closed with a Kel-F cap in a dry nitrogen atmosphere. The rotor was put into the probe and equilibrated at 80°C for 30 min. The magic angle spinning then began and the Bloch decay $^{13}$C spectra were collected.

### Characterizations

All NMR experiments were performed on a Varian Infinity-plus 400 spectrometer operating at a magnetic field strength of 9.4 T. The $^{13}$C resonance frequency at this field strength was 100.5 MHz. A Chemagnetics 5 mm MAS probe was employed to acquire all the spectra. The 90° pulse width for $^{13}$C was 2.6 µs. The recycle delay was 5 s for all the ex-situ experiments. For the in-situ capillary-breaking experiments, the $T_1$ of liquid benzene placed in the rotor with carbon nanotubes and the benzene adsorbed in the nanotubes at room temperature had been measured as 0.20 s and 0.14 s, respectively. Hence, the recycle delay was set as 1 s, which was valid for all states of benzene (5* $T_1$). The accumulation number was 2, so the time resolution was 2 s. $^{13}$C chemical shifts were referenced to hexamethylbenzene (HMB).

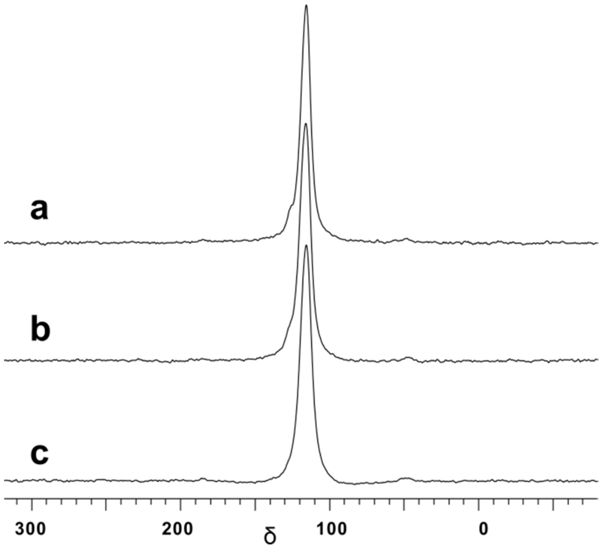

**Fig. 1.** $^{13}$C MAS NMR spectra of benzene adsorbed in DWNTs at (a) 80°C (b) RT (c) 7°C.

## Results and Discussion

The quality and morphology of the DWNTs sample has been demonstrated in the literature.[35] It was confirmed that the DWNTs sample had been well purified and contained little amorphous carbon. The typical inner diameters of the DWNTs were in the range of 1~1.5 nm (Fig. S1, ESI†). Ex-situ NMR experiments were performed first. Fig. 1 shows the $^{13}$C MAS NMR spectra of benzene adsorbed in DWNTs. A main peak at δ 115 together with a small shoulder at *ca*. δ 126 was found in the spectrum at room temperature. The $^{13}$C chemical shift of bulk benzene is at δ 128, while an up-field shift of the $^{13}$C NMR of methanol and the $^{1}$H NMR of $H_2O$ molecules endohedrally adsorbed in CNTs due to the strong diamagnetic shielding effect of nanotubes has been observed[20, 27]. Based on the chemical shift values, we tentatively assign the peak at δ 115 and the shoulder at δ 126 to benzene molecules in and out of the DWNTs, respectively. The intensity of the shoulder signal slightly increased when the temperature was raised to 80°C (Fig. 1a). In contrast, the shoulder peak disappeared when the temperature was lowered to 7°C (Fig. 1c). The nanotube interior sites have been found as high-energy adsorption sites of alkanes in experiments and simulation.[36] and the endohedral adsorption has been observed to reach a maximum with increased pressure by Wu et al. when they studied the methane and ethane adsorption in single-walled carbon nanotubes (SWNTs) using $^{1}$H NMR.[24] It also has been revealed that the endohedral adsorption is preferential in CNTs and the exohedral adsorption does not take place until the endohedral adsorption saturates.[27] Thus the main peak at δ 115 was unambiguously assigned to benzene endohedrally adsorbed in DWNTs and the shoulder peak at δ 126 was ascribed to benzene out of the DWNTs. When the temperature was increased, some benzene molecules in DWNTs gained energy to overcome the adsorption energy barrier to go out of the nanotubes and then the intensity of the shoulder peak increased; when the temperature was decreased, the nanotubes could accommodate more benzenes and the small quantity of benzene molecules out of the DWNTs entered into the nanotubes and then the shoulder peak disappeared. Although the benzene molecules in the DWNTs might exchange with the benzene molecules out of the DWNTs to some extent, two peaks respectively ascribed to benzene in and out of the nanotubes could still be well resolved in the $^{13}$C NMR spectra, and the chemical shift of the peaks did not change noticeably with temperature, showing that it was a slow exchange process on the NMR time scale and the affections of exchange could be ignored.

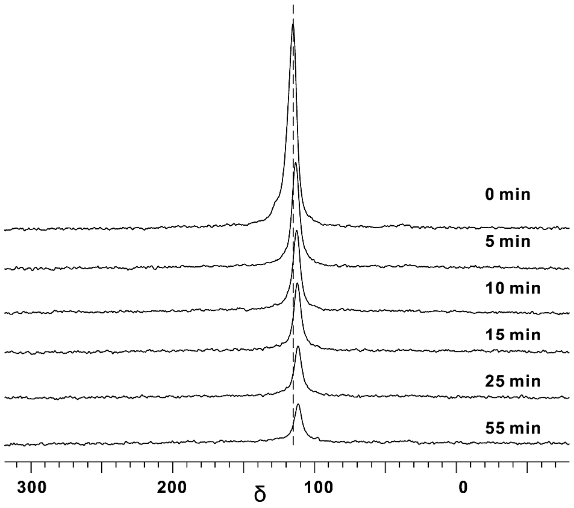

**Fig. 2.** $^{13}$C MAS NMR spectra of benzene adsorbed in DWNTs as a function of desorption time.

To confirm the assignment, desorption experiments were also performed. The cap of the NMR rotor was removed and the DWNTs adsorbed with benzene were exposed to the air. The benzene began to desorb from the DWNTs and the timing began from then on. The $^{13}$C MAS NMR spectra of benzene in DWNTs with different desorption time were recorded and shown in Fig. 2. The shoulder peak at δ 126 disappeared after desorption for 5 min, and the intensity of the main peak also decreased. It is in agreement with the fact that the benzene molecules out of DWNTs desorbed first and the desorption of the benzene molecules in DWNTs followed. The intensity of the $^{13}$C peak of benzenes in DWNTs further decreased with increasing the desorption time and the chemical shift gradually moved up-field. The chemical shift changed from δ 115 to δ 111 after desorption for 55 min. DFT study has shown that the magnetic shielding is homogeneously distributed inside nanotubes and the resulting chemical shift change of confined molecules in CNTs is almost independent of their relative location with respect to the CNTs wall, whilst nonbonded interactions of host−guest and guest−guest affect chemical shift significantly.[37] Hence, the up-field shift of the $^{13}$C peak of benzenes in DWNTs with desorption time might be resulted from the change in host−guest and guest−guest interactions when benzene molecules gradually desorbed from the nanotubes.

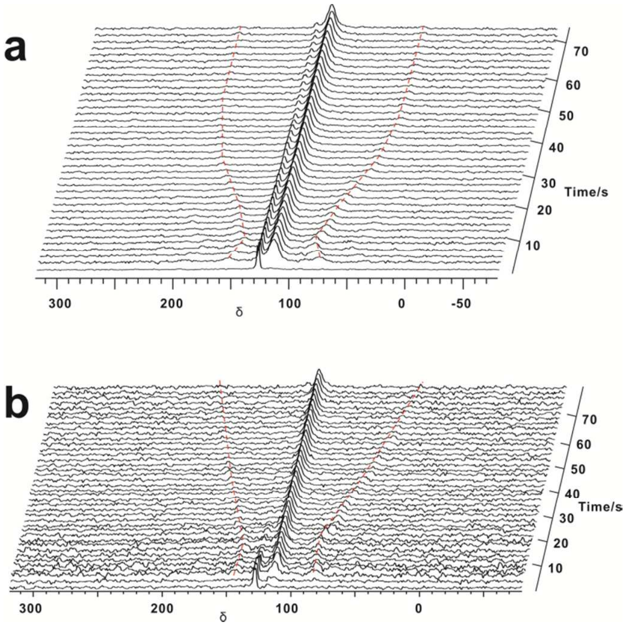

**Fig. 3.** In-situ $^{13}$C MAS NMR spectra recorded as a function of time during adsorption of benzene in DWNTs at (a) 7°C (b) 80°C. Dashed red lines indicate the spinning sidebands.

Then the in-situ capillary-breaking $^{13}$C NMR experiments were performed to study the adsorption process of benzene in DWNTs at the very earliest stages. $^{13}$C MAS NMR spectra were consecutively recorded to monitor the adsorption progress. Fig. 3a shows the in-situ $^{13}$C MAS NMR spectra recorded as a function of time during adsorption of benzene in DWNTs at 7°C. At first, there was only one $^{13}$C signal of bulk benzene centered at δ 128 with a J-coupling split in the spectrum. Then the glass capillary was broken during the accelerating period of the magic-angle spinning (at a speed of *ca*. 4 kHz deducing from the spinning sidebands) and the adsorption of benzene in DWNTs occurred. Another signal of benzene adsorbed in nanotubes appeared at δ 115 immediately after the breaking of the capillary. About 80% of the benzene molecules had been adsorbed into the DWNTs in the earliest 2 s, followed by a slow increase of the benzenes adsorbed in DWNTs (Fig. 4, obtained from the integral of $^{13}$C peak at δ 115 with its spinning sidebands included). When the benzene was released from the glass capillary and contacted the DWNTs at 7°C, it was still liquid. The capillary effect of the carbon nanotubes make the earliest adsorption process so fast that little kinetic information could be extracted from the spectra. The experiment had also been performed at room temperature and similar results were obtained (spectra not shown). Then the temperature was increased to 80°C and the spectra as a function of adsorption time were shown in Fig. 3b. The intensity of the peak at δ 115 increased with adsorption time whilst that at δ 128 decreased. The amount of benzene in and out of DWNTs as a function of adsorption time was shown in Fig. 4. The amount of benzene adsorbed in DWNTs increased rapidly at the early stage and then grew slowly. Actually, the adsorption process of benzene was a dynamic state made up of two opposing process, the adsorption and desorption.

$$\text{Benzene} + \text{DWNTs} \rightleftharpoons \text{Benzene@DWNTs}$$

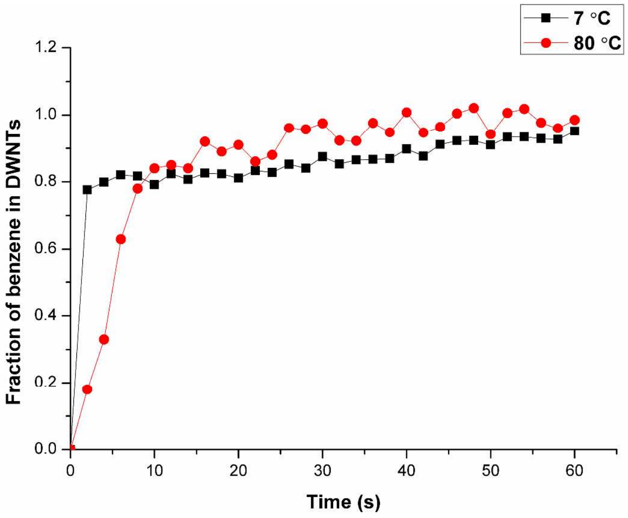

**Fig. 4.** Fraction of benzene in DWNTs as a function of adsorption time.

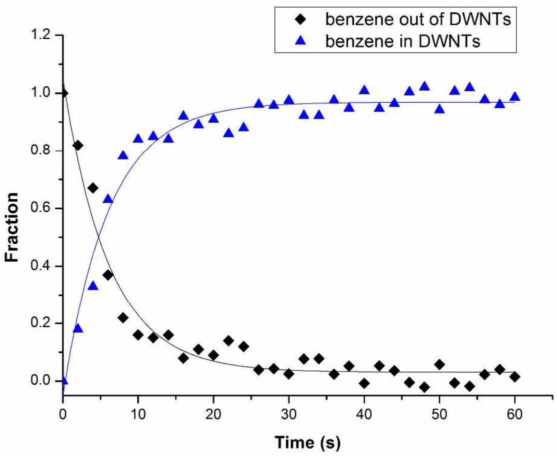

**Fig. 5.** Exponential fittings of the fraction of benzene in and out of DWNTs as a function of adsorption time.

Where Benzene@DWNTs stands for benzene adsorbed in DWNTs. The rate of adsorption is taken to be just proportional to the pressure and the number of the bare sites:

$$v_{ads} = k_1 p(1 - \theta) \qquad (1)$$

where $v_{ads}$ is the rate of adsorption, $\vartheta$ is the fraction of occupied adsorption sites and thus (1-$\vartheta$) is the fraction of bare sites in DWNTs, $k_1$ is the rate constant of adsorption and $p$ is the pressure. Here the experiment was performed at 80°C, a temperature of the boiling point of benzene. In the NMR rotor, the liquid benzene was fast vaporized to gas phase to compensate the decrease of pressure caused by adsorption before *ca*. 10 s. After this time, liquid benzene is almost completely vaporized. However, we have tested that the adsorption in DWNTs has already been near saturation and the pressure would not drop significantly. So we can approximately presume that the pressure $p$ in equation (1) could be considered as constant during the whole adsorption process. The rate of desorption is proportional to the number of occupied adsorption sites:

$$v_{des} = k_2 \theta$$

Where $v_{des}$ is the rate of desorption and $k_2$ is the rate constant of desorption. The differential rate for the process is

$$\frac{d\theta}{dt} = v_{ads} - v_{des} = k_1 p(1 - \theta) - k_2 \theta$$

Rearrangement gives

$$\frac{d\theta}{\theta - \dfrac{k_1 p}{k_1 p + k_2}} = -(k_1 p + k_2)dt$$

Integrating both sides, we find

$$\int_0^\theta \frac{d\theta}{\theta - \dfrac{k_1 p}{k_1 p + k_2}} = -(k_1 p + k_2)\int_0^t dt$$

or

$$\ln \frac{a-\theta}{a} = -bt$$

Where $a = k_1 p / (k_1 p + k_2)$ and $b = k_1 p + k_2$ .

Exponentiation of both sides gives

$$\theta = a[1 - \exp(-bt)]$$

Considering errors caused by other uncontrollable factors, such as capillary condensations, a constant *c* was introduced to correct the equation.

$$\theta = a[1 - \exp(-bt)] + c$$

or

$$\theta = -a * \exp(-bt) + d$$

Where $d = a + c$ . So the fraction of occupied adsorption sites or the amount of benzene in DWNTs should increase exponentially with the adsorption time. Similarly, the amount of benzene out of DWNTs should decrease exponentially. The results of simulations were shown in Fig. 5. The kinetic curves of benzene in and out of DWNTs could be fitted well with an exponential growth and exponential decay function, respectively. The adsorption in the DWNTs was near completion within 10 s, and we directly observed the kinetics of such a fast adsorption process in CNTs by using in-situ solid-state NMR technique. However, we failed to simulate the kinetic curves of the adsorption at 7 $^{o}$C using an exponential or biexponential function, showing the limitations of our experiments for a quantitative evaluation of the adsorption kinetics.

## Conclusions

In summary, in-situ solid-state $^{13}$C NMR was employed for the first time to monitor the adsorption process of benzene in DWNTs at the very earliest stages. The results reveal that two $^{13}$C NMR peaks were observed and ascribed to benzenes in and out of DWNTs, respectively, when benzene was adsorbed in DWNTs. The evolution of adsorption was directly and successfully observed by using the in-situ capillary-breaking $^{13}$C NMR method. The adsorption process was fast (of the order of several seconds) and the kinetics of the adsorption process was obtained by integrating the $^{13}$C peaks as a function of adsorption time. The kinetic could be interpreted with a model of opposing adsorption-desorption process and the kinetic curves could be satisfyingly fitted by an exponential function. However, there are limitations of this method. It could not be used to simulate the kinetic curves of the adsorption at 7 $^{o}$C. To evaluate its adsorption kinetics quantitatively, faster in-situ techniques should be developed.

## Acknowledgements

This study was supported by the National Natural Science Foundation of China (21103183), China Postdoctoral Science Foundation (20110491547) and High-level Talent Foundation of Henan University of Technology (2012BS032, 2012BS059 and 2015QNJH10). The authors are very grateful to Prof. Xinhe Bao, Xiuwen Han and Xiulian Pan in Dalian Institute of Chemical Physics, Chinese Academy of Sciences, for inspirational and valuable discussions.

## Notes and references

1.T. Ando, *NPG Asia Mater.*, 2009, **1**, 17.

2.Jan M. Schnorr and T. M. Swager, *Chem. Mater.*, 2011, **23**, 646.

3.X. Liu, M. Wang, S. Zhang and B. Pan, *J. Environ. Sci.*, 2013, **25**, 1263.

4.M. Mittal and A. Kumar, *Sens. Actua. B-Chem.*, 2014, **203**, 349.

5.P. Serp and E. Castillejos, *ChemCatChem*, 2010, **2**, 41.

6.X. Pan and X. Bao, *Chem. Commun.*, 2008, 6271.

7.X. Pan and X. Bao, *Acc. Chem. Res.*, 2011, **44**, 553.

8.P. Kondratyuk and J. T. Yates, *Acc. Chem. Res.*, 2007, **40**, 995.

9.J. Guan, X. Pan, X. Liu and X. Bao, *J. Phys. Chem. C*, 2009, **113**, 21687.

10.H. Zhang, X. Pan, X. Han, X. Liu, X. Wang, W. Shen and X. Bao, *Chem. Sci.*, 2013, **4**, 1075.

11.G. Mestl, N. I. Maksimova, N. Keller, V. V. Roddatis and R. Schlogl, *Angew. Chem., Int. Ed.*, 2001, **40**, 2066.

12.J. Zhang, X. Liu, R. Blume, A. Zhang, R. Schlögl and D. Su, *Science*, 2008, **322**, 73.

13.S. Vasenkov, W. Bohlmann, P. Galvosas, O. Geier, H. Liu and J. Karger, *J. Phys. Chem. B*, 2001, **105**, 5922.

14.S. F. Stallmach, S. Groger, V. Kunzel, J. Karger, O. M. Yaghi, M. Hesse and U. Muller, *Angew. Chem., Int. Ed.*, 2006, **45**, 2123.

15.R. Mueller, R. Kanungo, M. Kiyono-Shimobe, W. J. Koros and S. Vasenkov, *Langmuir*, 2012, **28**, 10296.

16.S. Xu, W. Zhang, X. Liu, X. Han and X. Bao, *J. Am. Chem. Soc.*, 2009, **131**, 13722.

17.M. Xu, K. D. M. Harris, J. M. Thomas and D. E. W. Vaughan, *ChemPhysChem*, 2007, **8**, 1311.

18.M. Xu, K. D. M. Harris and J. M. Thomas, *J. Am. Chem. Soc.*, 2008, **130**, 5880.

19.P. Huang, E. Schwegler and G. Galli, *J. Phys. Chem. C*, 2009, **113**, 8696.

20.W. Sekhaneh, M. Kotecha, U. Dettlaff-Weglikowska and W. S. Veeman, *Chem. Phys. Lett.*, 2006, **428**, 143.

21.Q. Chen, J. L. Herberg, G. Mogilevsky, H. Wang, M. Stadermann, J. K. Holt and Y. Wu, *Nano Lett.*, 2008, **8**, 1902.

22.D. Sebastiani and K. N. Kudin, *ACS Nano*, 2008, **2**, 661.

23.E. Zurek and J. Autschbach, *Int. J. Quantum Chem.*, 2009, **109**, 3343.

24.S. A. Kleinhammes, S. Mao, X. Yang, X. Tang, H. Shimoda, J. Lu, O. Zhou and Y. Wu, *Phys. Rev. B*, 2003, **68**, 075418.

25.K. Matsuda, T. Hibi, H. Kadowaki, H. Kataura and Y. Maniwa, *Phys. Rev. B*, 2006, **74**, 073415.

26.R. J. Anderson, T. P. McNicholas, A. Kleinhammes, A. Wang, J. Liu and Y. Wu, *J. Am. Chem. Soc.*, 2010, **132**, 8618.

27.X. Liu, X. Pan, W. Shen, P. Ren, X. Han and X. Bao, *J. Phys. Chem. C*, 2012, **116**, 7803.

28. C. Goze-Bac, S. Latil, P. Lauginie, V. Jourdain, J. Conard, L. Duclaux, A. Rubio and P. Bernier, *Carbon*, 2002, **40**, 1825.

29.S. Hayashi, F. Hoshi, T. Ishikura, M. Yumura and S. Ohshima, *Carbon*, 2003, **41**, 3047.

30. Y. Kim, E. Abou-Hamad, A. Rubio, T. Wagberg, A. V. Talyzin, D. Boesch, S. Aloni, A. Zettl, D. E. Luzzi and C. Goze-Bac, *J. Chem. Phys.*, 2010, **132**, 021102.

31. J. C. C. Freitas, F. G. Emmerich, G. R. C. Cernicchiaro, L. C. Sampaio and T. J. Bonagamba, *Solid State Nucl. Magn. Reson.*, 2001, **20**, 61.

32.E. G. Nikolaev, O. E. Omel'yanovskii, V. S. Prudkovskii, A. V. Sadakov and V. I. Tsebro, *Low Temp. Phys.*, 2009, 123.

33.E. Abou-Hamad, M. R. Babaa, M. Bouhrara, Y. Kim, Y. Saih, S. Dennler, F. Mauri, J. M. Basset, C. Goze-Bac and T. Wagberg, *Phys. Rev. B*, 2011, **84**, 165417.

34.H. Yu, Q. Zhang, Q. Zhang, Q. Wang, G. Ning, G. Luo and F. Wei, *Carbon*, 2006, **44**, 1706.

35.H. Zhang, X. Pan, J. Liu, W. Qian, F. Wei, Y. Huang and X. Bao, *ChemSusChem*, 2011, **4**, 975.

36.P. Kondratyuk, Y. Wang, J. K. Johnson and J. T. Yates, *J. Phys. Chem. B*, 2005, **109**, 20999.

37.P. Ren, A. Zheng, X. Pan, X. Han and X. Bao, *J. Phys. Chem. C*, 2013, **117**, 23418.